

## CHEMICAL AND MINERALOGICAL ANALYSIS OF REFORMED SLAG DURING IRON RECOVERY FROM COPPER SLAG IN THE REDUCTION SMELTING

Copper slag is usually a mixture of iron oxide and silicon dioxide, which exist in the form of fayalite ( $2\text{FeO}\cdot\text{SiO}_2$ ), and contains ceramic components as the  $\text{SiO}_2$ ,  $\text{Al}_2\text{O}_3$  and  $\text{CaO}$  depending on the initial ore quality and the furnace type. Our present study was focused on manufacture of foundry pig iron with Cu content from copper slag using high-temperature reduction smelting and investigate utilization of by-products as a reformed slag, which is giving additional value to the recycling in a replacement of raw material of Portland cement. Changes of the chemical and mineralogical composition of the reformed slag are highly dependent on the  $\text{CaO}$  concentration in the slag. The chemical and mineralogical properties and microstructural analysis of the reformed slag samples were determined through X-ray Fluorescence spectroscopy, X-Ray diffractometer and Scanning Electron Microscopy connected to the dispersive spectrometer studies.

*Keywords:* Copper slag, fayalite, pig iron, reformed slag

### 1. Introduction

Copper slag is generated as a by-product formed in copper manufacturing processes, it have been the subject of research for recycling in a wide range of possible applications. In copper smelting industry, 2.2 to 3 tons of the copper slag is generated from the process of smelting per ton of copper production, and 1.5 million tons of copper slag is generated in South Korea every year [1-5]. Dumping or disposal of copper slag causes wastage of metal values and leads to environmental problems. In particular, the dumping requires wide area and leads to many impacts such as eroding and damaging the land surface, solid and gas substances polluting the atmosphere [6]. In actually, South Korea is a small land country with a high population. Therefore, South Korea refuses to landfill the metallurgical slags and promotes zero waste through the re-use and recycling of these waste materials. Recently, some scientists all over the world had paid special attention to recycle copper slag and developed several technologies that can be decreased the cost of the products and eliminated the costs of disposal of the copper slag. Although South Korea has been challenging to utilize the copper slag in diversified ways like recovery value metals and preparation of cement replacement in concrete, there is copper slag is only used in agent for roadbed and additives for concrete [5].

The copper slag is usually a mixture of iron oxide and silicon dioxide, which exist in the form of fayalite ( $2\text{FeO}\cdot\text{SiO}_2$ ), and contains ceramic components as the  $\text{SiO}_2$ ,  $\text{Al}_2\text{O}_3$  and  $\text{CaO}$  depending on the initial ore quality and the furnace type. Although the ceramic components as the  $\text{SiO}_2$ ,  $\text{CaO}$  and  $\text{Al}_2\text{O}_3$  in copper slag are a higher-value partial substitute in cement, the copper slag is only considered as the raw material for as a Portland cement replacement of iron ore that it was studied by I.Alp and Arino-Morena [7-9] due to its high amount of iron content and fayalite phase.

In the copper slag, a large amount of iron is typically contained about 40% Fe, and small amount copper about 1%, it can be considered as a raw material of iron [10]. The utilization of copper slag for construction replacement area is not efficiently recycling method, there is value metals as Fe, Cu and minor amounts of the Zn, Ti, Co and precious metals are contained in the copper slag. Many studies have been conducted to recover the iron, copper and valuable metals from the copper slag by hydrometallurgical, pyrometallurgical and physicochemical treatment depending on the metals to be recovered. Hydrometallurgical treatment is widely used in copper recovery from copper slag that including direct leaching in sulphuric acid, leaching in sulphuric acid through  $\text{H}_2\text{S}$  gas or ferric chloride [11], which are used on the recovery of nonferrous metals as the Cu, Co, Mo,

<sup>1</sup> PUKYONG NATIONAL UNIVERSITY, DEPARTMENT OF METALLURGICAL ENGINEERING, BUSAN, REPUBLIC OF KOREA

\* Corresponding author: jpwang@pknu.ac.kr





## 2.2. Experimental apparatus and sample preparation

The reduction smelting for sample preparation was performed in a 10 KW, 30 KHZ High-Frequency Induction Furnace with melt size 10 kg of steel. The high-frequency induction furnace consisted of a cooler, controller and heater box. The installation space was small and the additional equipment such as dust collector was miniaturized to reduce the difficulty and cost of the process. The temperature of the high-frequency induction melting furnace was controlled by regulating the voltage.

Fig. 2 is a schematic diagram of a heater box where high-frequency induction is used in the experiment. The heater box enclosed the equipment and eliminated dust and flue gases from the furnace. Argon gas was released into the heater box to maintain an inert atmosphere. Electricity was conducted through the thermo-generator using the graphite crucible. Then the crucible was placed inside the heater box and the temperature was measured using a thermocouple.

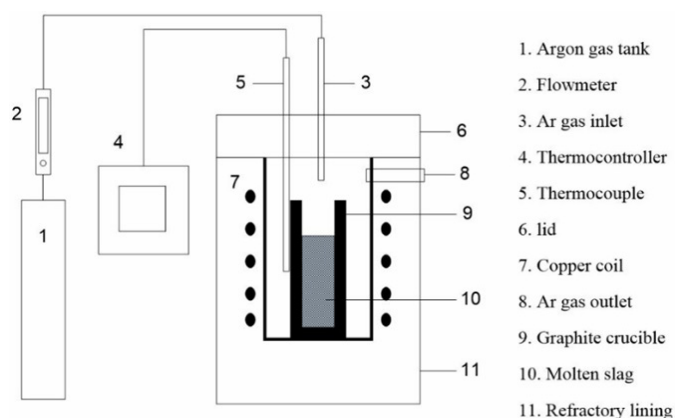


Fig. 2. Schematic diagram of experimental apparatus

In the experimental process, the copper slag with irregular fine irregularities of 1 mm to 3 mm and reducing agent activated carbon were mixed with the sample at the ratio of 9 g per 100 g and then charged into the carbon crucible. CaO additives were 5, 10, 15, 20 and 25 g per 100 g of copper slag under the ratio  $B = \text{CaO (wt.\%)} / \text{SiO}_2 \text{ (wt.\%)} = 0.8, 0.9, 1.0, 1.1 \text{ and } 1.2$ . The mixture was put into a carbon crucible, and then the carbon crucible was placed inside the box of the high-frequency induction furnace. The experiment was heated up to the necessary temperature of 1600°C for 40 minutes and reduction smelting process continued for 30 minutes of holding. Then, the sample was left inside the furnace to cool down to room temperature naturally.

## 2.3. Experimental methods

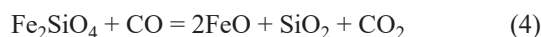
For chemical and mineralogical analysis, the reformed slag samples were used the powdered samples for mixing with an equal amount in a homogeniser. The chemical compositions of the reformed slag were determined using X-Ray fluorescence spectroscopy. XRF analysis was carried out in average results

taken. Mineralogical analysis of the reformed slag samples was examined at room temperature using X-ray diffractometer with 5°-90° (2θ) and step size of 0.02°. Finally, for micro-analysis, the reformed slag samples were treated applying a standard method, which is grinding and polishing, to prepare metallographic scratch patterns. The performed micro-analysis of the reformed slag also included the scanning electron microscopy (SEM) connected to the dispersive spectrometer (EDS).

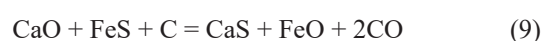
## 3. Results and discussions

### 3.1. Consideration of smelting reduction of copper slag

The present experiment was performed to produce the low Sulphur foundry pig iron with copper using carbon reduction smelting with CaO additives at the high temperature of 1600°C for 30 minutes. In the reduction smelting of copper slag, direct reduction with solid carbon and indirect reduction with CO gas are observed. During the reduction process, solid carbon converts to CO gas by the following reaction of 1 to 3 at temperatures above 900°C [20]. Subsequently, while the fayalite ( $2\text{FeO} \cdot \text{SiO}_2$ ) in copper slag started to decompose at the high temperature, the decomposed iron oxide from the fayalite compound is reduced by reduction agents according to the following reactions of 4 to 7.



The added CaO supports the decomposition of the fayalite and influences on the reduction of iron oxide by the following reaction of 8, and CaO of right amount influences on the forming of basic slag with a high content of CaO, and hence the basic slag can be dissolved the sulphur from the recovered pig iron in the reducing process as shown in reactions 9 and 10. In this case, it might be seen that the remaining oxides as the  $\text{SiO}_2$ , CaO,  $\text{Al}_2\text{O}_3$  and MgO interact with each other, and hence generate the reformed slag. The reformed slag might consist of the considering typically eutectic compounds as the  $\text{CaO} \cdot \text{SiO}_2$ ,  $2\text{CaO} \cdot \text{SiO}_2$ ,  $3\text{CaO} \cdot 2\text{SiO}_2$ ,  $\text{CaO} \cdot \text{Al}_2\text{O}_3 \cdot 2\text{SiO}_2$ ,  $2\text{CaO} \cdot \text{Al}_2\text{O}_3 \cdot \text{SiO}_2$ ,  $\text{CaO} \cdot \text{MgO} \cdot \text{SiO}_2$ , etc.



Copper oxide in the copper slag can be easily reduced and dissolved in the molten metal phase, and also zinc oxide

is reduced to volatile zinc, which is removed from the furnace with as the fumes, by carbon at a temperature of 980~1000°C during the reduction process. It was confirmed that the chemical analysis had shown the copper and zinc did not present in the reformed slag, as shown in Table 2.

Reduction behaviour of iron oxide to be reduced from fayalite decomposition was examined by thermodynamic analysis using HSC 5.1 chemistry software. It determined that as the results of the thermodynamic analysis in Fig. 3, iron can be reduced from the decomposition of fayalite in reduction smelting process at high temperatures, and moreover, due to impact of CaO, reduction of iron in fayalite is more intensified. As above illustrated, reduction CuO can be reduced by CO gas at all temperatures, it is shown in Fig. 3.

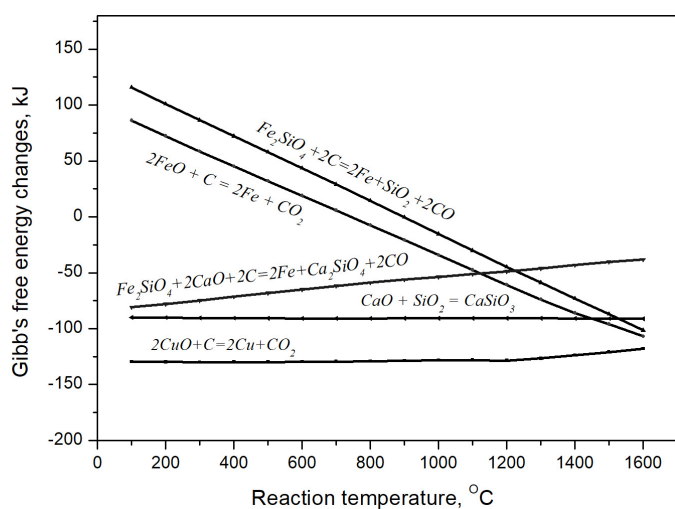


Fig. 3. Gibb's free energy changes of reduction of components in copper slag by reducing carbon

### 3.2. Reduction smelting for recovery Fe-Cu alloy

In reduction smelting experiment with carbon additives, Fe and Cu reduced from the slag and then formed to a metal phase, where are separated by the specific gravity difference with slag consisting of SiO<sub>2</sub>, CaO, Al<sub>2</sub>O<sub>3</sub> and etc at 1600°C for 30 minutes of holding. Table 2 shows the EDS results of the chemical composition of the pig iron with copper recovered from the copper slag by high-temperature reduction according to the CaO additives at a reaction temperature of 1600°C for 30 minutes of holding time. It was observed that there were no significant differences on the Fe and Cu content in pig iron with copper according to the CaO additives, which were about 86 wt.% of Fe and 3 wt.% of Cu, that indicating the formation of Fe-Cu alloy. But, when carbothermal reduction without CaO in the previous study, sulphur content in the pig iron was a higher amount of 0.46 than carbothermal reductions with CaO additives that as over 15 g of CaO additives, the sulphur content in the ferrous was decreased the lower amount of 0.001%. It confirmed that reformed slag was completely dissolved the sulphur from pig iron according to the desulphurization principle.

TABLE 2

Chemical composition of the pig iron recovered from copper slag

Type Si	Element, wt.%							
	C	Cr	Mn	Cu	Fe	S		
Without CaO additives	2.94	4.13	1.25	0.81	2.93	87.45	0.49	
With CaO additives, wt.%	5	4.56	3.95	1.12	1.82	3.01	85.54	0.041
	10	4.10	4.09	1.03	1.56	3.17	86.05	0.025
	15	4.23	4.35	1.25	1.27	3.19	85.71	0.001
	20	3.63	3.95	0.87	1.30	3.06	87.19	0.001
	25	2.94	4.62	1.25	0.81	2.93	87.45	0.001

Cast irons are widely used multicomponent ferrous alloy, that obtained in place of steel at considerable low cost and optimum combination properties as the castability, machinability, excellent wear resistance and high hardness and high inherent damping capabilities. It is known that adding alloy elements, cooling rate and formation of graphite influence the properties of the cast iron. Copper leads to graphitizing and pearlitization, which phase-stabilizing, of the cast iron that affects substantially mechanical properties such as strength, toughness and corrosion resistance [16,21-23]. Many researchers studied the effect of Cu addition on the mechanical properties and structure formation of cast iron. A.Es. Nassef et al. [21], J.O. Agunsove et al. [24] and A.A. Razumakov et al. [22] have concluded the structure and mechanical properties of cast iron are affected by copper addition of 1 to 3.5% that resulted in better wear resistance and lowest wear loss, hardness and tensile strength initially increased according to the volume fraction of graphite decreased and stabilization of pearlite. Cast iron is contained main elements such as carbon ranging from 1.8 to 4% and silicon 1 to 3%, and other alloying elements as the copper of about 2.0. In the carbothermal reduction smelting, the recovered pig iron were appeared as the cast iron according to the content-ranges of C and Si presented about 4.2 wt.% and 4.0 wt.% in the pig iron recovered from the copper slag, respectively, consequently, it was considered the recovered pig iron with copper can be used through in place of cast iron ingots.

### 3.3. Chemical analysis of reformed slag

Table 3 shows that the chemical composition of the reformed slag as determined by the X-ray Fluorescence. As shown results of the chemical composition of the reformed slag without CaO additives, it was found that the Fe<sub>2</sub>O<sub>3</sub> content was not detected, which is indicating that Fe was completely recovered, whereas SiO<sub>2</sub> content was increased. The reformed secondary slag contained about 46 wt.% SiO<sub>2</sub>, 26 wt.% CaO and 14 wt.% Al<sub>2</sub>O<sub>3</sub>, and it was an acid slag. It was observed the acid reformed slag.

On the other hand, in the reduction smelting with CaO additives, the SiO<sub>2</sub> content in the reformed slag was decreased according to the CaO additives, and hence CaO content in the reformed slag was increased, but Fe<sub>2</sub>O<sub>3</sub> was contained at small



TABLE 3

Chemical composition of reformed slag

Element, wt. %	SiO <sub>2</sub>	CaO	Al <sub>2</sub> O <sub>3</sub>	MgO	Na <sub>2</sub> O	TiO <sub>2</sub>	K <sub>2</sub> O	MnO	SO <sub>3</sub>	BaO	Fe <sub>2</sub> O <sub>3</sub>	SrO	P <sub>2</sub> O <sub>5</sub>
Typical BFS	30 to 38	32 to 50	7 to 15	5 to 15	~0.5	—	~0.5	0.2 to 1.0	1-2	—	0.1 to 1.5	—	<0.2
Reformed slag without CaO	46.25	26.57	14.49	3.92	2.70	0.72	0.99	1.70	0.05	0.9	ND	0.86	0.90
Reformed slag with CaO additives, wt. %	5	40.05	37.50	13.45	5.00	1.52	0.91	0.635	0.61	0.30	—	—	—
	10	37.42	42.54	13.12	4.40	0.54	0.41	0.18	0.23	0.28	0.66	0.10	0.07
	15	31.80	50.86	12.42	4.14	—	0.24	—	—	0.46	—	—	0.08
	20	31.82	50.94	11.80	3.49	—	0.21	—	—	0.45	0.49	0.70	0.07
	25	22.36	60.91	11.24	3.50	—	—	—	—	0.55	—	1.14	—

rates of 0.10 to 1.14 wt.%, as shown in Table 3. In this case, the basicity CaO/SiO<sub>2</sub> ratio of the reformed slag has been increased at 1.07, 1.26, 1.70, 1.71 and 2.9 due to increasing the CaO content in the reformed slag, and basicity affected significantly the sulphur capacity.

Portland cement is manufactured through a closely controlled chemical combination of Ca, Si, Al, Fe and other ingredients, that common materials for cement include limestone, shells, and chalk or marl combined with shale, clay, blast furnace slag, silica sand, and iron ore. As the blast furnace slag (BFS) is one of massive raw material acquired Portland blast furnace slag cement (PBFSC), which mixed ground BFS and Portland cement, because of BFS has a similar chemical composition with the chemical composition of Portland cement [25-28]. For manufacture Portland cement, limestone as the principal raw material is burned at a high temperature caused air pollution, which large CO<sub>2</sub> emissions, therefore, BFS was discovered a partial replacement in raw material of Portland cement due to PBFSC could be a kind of eco-friendly cement emits about less 40% of CO<sub>2</sub> than Portland cement supported by Green Purchasing law [25-28]. Thus, alkaline-activated cement as the PBFSC with alkali activators such as sodium hydroxide, sodium silicate and sodium carbonate are similar and greater properties to Portland cement, and alkaline-activated cement is produced at room temperature that it can be reduced the Portland cement cost and CO<sub>2</sub> emissions by 80-86% [26]. South Korea has been also used the BFS in replacement of the raw material of Portland cement and widely employed in civil engineering structures due to its eco-friendly processing and lower cost of PBFSC. The qualities of PBFSC are specified in KS L 5210: Blast furnace slag cement of Korean standard, there are three types that 1 type is over 5, less than 30 of BFS ratio, 2 types (over 30, less than 60) and 3 type (over 60, less than 70). In 2017s in South Korea, the BFS has been generated about 16 million tons a year that 92% of BFS used in cement industry [29]. Therefore, present work was attempted to produce reformed slag with similar behaviours as the BFS from copper slag during iron recovery. When the CaO additives are over 10 to 20 wt.%, the chemical compositions of reformed slag observed similar chemical composition of the Blast Furnace slag (BFS). Chemical analysis both of the produced slag and Blast-Furnace slag show that the major oxides as the CaO, SiO<sub>2</sub>, MgO and Al<sub>2</sub>O<sub>3</sub> are contained up about 95% of the total in accordance with requirements of BFS for cement material, as shown in Ta-

ble 3. It was observed that produced slag with over 10 to 20 wt.% of CaO additives is achievable as a raw material for PBFSC.

### 3.4 .Mineralogical analysis

The chemical components of reformed slag were obtained by identification of precipitated crystalline phases with powder X-ray diffraction analysis (XRD). As shown in Fig. 4(a), glass-like and quartz phases are presented in the reformed slag sample without CaO additives, it is indicated that slag was like glass. When the CaO additives is 5 wt.%, diffraction peaks of the glass-like slag weren't detected and glass-like slag has been transformed into diopside aluminian Ca(Mg)(Al,Si)SiO<sub>7</sub> and akermanite-gehlenite series Ca<sub>2</sub>(Al,Mg)(Si,Al)SiO<sub>7</sub> in which indicating that glass slag has been completely formed to calcium silicate phases, as shown in Fig. 4(b). As reformed slag with 10 wt.% CaO, akermanite-gehlenite series still appeared, but the diopside aluminian was transformed into calcium aluminosilicate Ca<sub>2</sub>Al<sub>2</sub>SiO<sub>7</sub>. When the CaO additives are of 15 and 20 wt.%, only akermanite-gehlenite series was observed, but at the CaO additives is of 25 wt.%, diffraction peaks of the gehlenite still appear while dicalcium silicate Ca<sub>2</sub>SiO<sub>4</sub> is also observed. It is indicated that dicalcium silicate phases are produced due to the increase of CaO concentration. To summarize, the glass-like slag was can be greatly transformed into new kind phases of calcium silicate when CaO additives are above 5 wt.%.

### 3.5. Microstructural analysis

For the microstructure analysis observation, reformed slag samples with polished were determined using scanning electron microscopy (SEM). The chemical composition of each phase of reformed slag was examined using energy dispersed X-ray (EDS). SEM images and EDS results are shown in Figs. 5-7, and Tables 4-6, respectively. Phase equilibria in the ternary oxide system Al<sub>2</sub>O<sub>3</sub>-CaO-SiO<sub>2</sub> and quaternary oxide system Al<sub>2</sub>O<sub>3</sub>-CaO-SiO<sub>2</sub>-MgO [30,31] is directly related to reformed slags.

As shown in Fig. 5(a), the microstructure of the reformed slag sample without CaO additives seemed like glass bulk matrix. Thus the glass matrix contains irregular crystal disperses, which

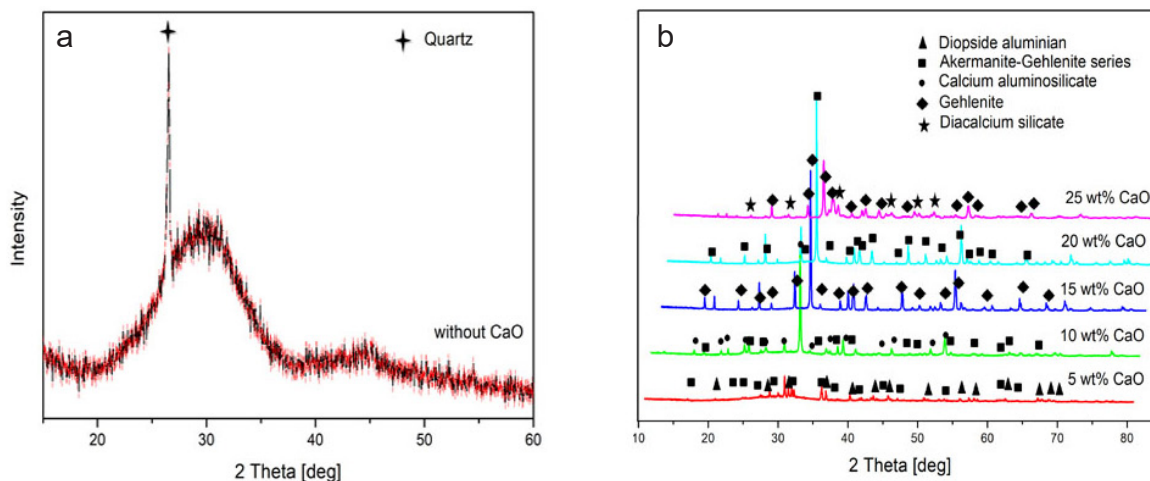


Fig. 4. Analysis of X-ray diffraction as a function of CaO additives on the reformed slag samples. (a) and (b) – reformed slag without and with CaO additives. Quartz-SiO<sub>2</sub>, diopside aluminian-Ca(Mg)(Al,Si)SiO<sub>7</sub>, calcium aluminosilicate-Ca<sub>2</sub>Al<sub>2</sub>SiO<sub>7</sub>, Gehlenite-Ca<sub>2</sub>(Al,Mg)(Si,Al)SiO<sub>7</sub>; akermanite-Ca<sub>2</sub>MgSi<sub>2</sub>O<sub>7</sub>; dicalcium silicate-Ca<sub>2</sub>SiO<sub>4</sub>

is spinel crystals, are Ti concentrating phase according to EDS analysis as shown in Fig. 5(c) and Table 4.

In the EDS analysis, the main constituent elements were measured as slag components of 22 wt.% Si, 19.5 wt.% Ca, 8.3 wt.% Al and 3.1 wt.% Mg, but Fe was not detected in the glass matrix, it was confirmed according to the result of the XRF analysis of the reformed slag without CaO additives as shown in Table 4. The glass matrix was as the pyroxene phase (Ca,Na)(Al,Mg)(Al,Si)<sub>2</sub>O<sub>6</sub> according to the EDS analysis and ternary oxide system of Al<sub>2</sub>O<sub>3</sub>-CaO-SiO<sub>2</sub>.

In the reformed slags with CaO additives, various solid-phases with different size and shape, and matrix are observed, as shown in Figs. 6-7. With CaO additives of 5 wt.%, the glass matrix of reformed slag without CaO additives transformed to calcium silicate matrix. The silicate matrix was contained about 26 wt.% of Ca, about 17 wt.% of Si, about 11 wt.% of Al and 3 wt.% of Mg, and it was such as the melilite Ca<sub>2</sub>(Al,Mg)[(Si,Al)SiO<sub>7</sub>] according to the SEM-EDS analysis and quaternary oxide system of Al<sub>2</sub>O<sub>3</sub>-CaO-SiO<sub>2</sub>-MgO. The solid-phases of anorthite series with coarse dendrite-like forms and Ti-spinels (Fig. 6 (e))

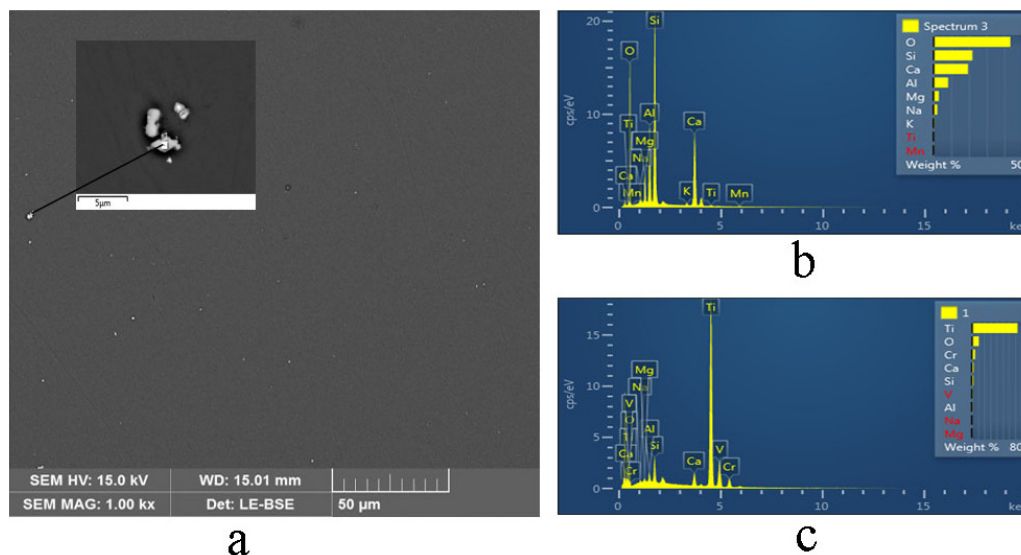


Fig. 5. SEM image and EDS micrographs of reformed slag sample without CaO additives: (a) glass matrix, (b) and (c) elemental analysis of glass matrix and spinels

TABLE 4

Results of EDS analysis on reformed slag without CaO additives

Element, wt.%	O	Si	Ca	Al	Mg	Na	Ti	Cr	V	Mn	K
Glass slag (Pyroxene)	43.42	22.02	19.56	8.30	3.10	2.23	0.40	—	—	0.38	0.55
1_Ti-spinel	11.34	2.76	2.89	1.19	0.34	0.41	74.16	5.32	1.58	0.34	—

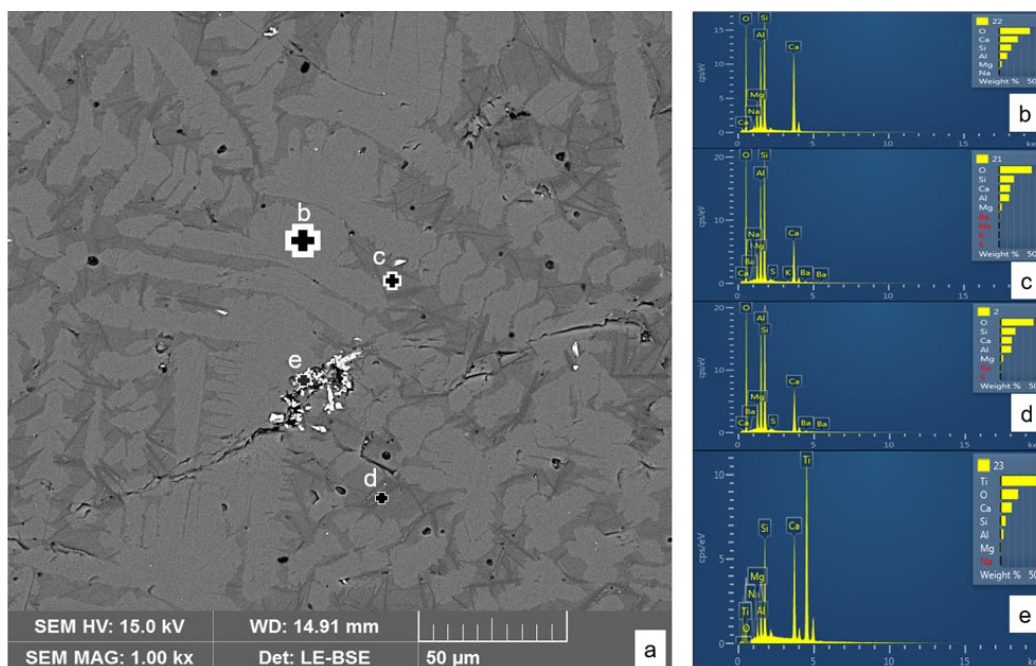


Fig. 6. SEM image and EDS micrographs of reformed slag sample with 5 wt.% CaO additives: (a) typical SEM image of reformed slag with 5 wt.% CaO, (b) elemental analysis of slag matrix; (c) solid-phases; (d) needles of solid-phases; and (e) spinels

were observed in the silicate matrix, where is still segregated, as shown in Fig. 6(a)-(e).

The solid-phases of irregular shape (Fig. 6(c)) and needle shape in the matrix (Fig. 6(d)) were similar chemical compositions according to the examination of EDS surface analysis, although they have the different shapes between the irregular solid-phase and needle solid-phase causing small amount of Na was contained in the irregular solid-phases, it is shown in Ta-

ble 5. In the EDS result, the solid-phases in the kind of anorthite have been contained about 0.15 wt.% of sulphur. In the case, the reformed slag can be dissolved the sulphur from molten metal.

When the CaO additives increased at 10 wt.%, the solid-phases still existed anorthite, but sharp shapes of the solid-phase were changed to large irregular particles with sharp angles, and transformed the melilite matrix to the anorthite series  $(Ca,Na)Al_2Si_2O_8$ , as shown in Fig. 7(a) and Table 6. As CaO additives

TABLE 5

Results of EDS analysis on reformed slag with 5 wt.% CaO additives

Element, wt.%	O	Si	Ca	Al	Mg	Na	Ti	K	Ba	S
<b>b_Melilite</b>	42.35	16.68	25.79	11.02	3.51	0.65	—	—	—	—
<b>c_Anorthite(Na)</b>	44.82	20.44	15.12	13.85	3.66	0.26	—	0.22	1.45	0.16
<b>d_Anorthite</b>	44.96	20.34	15.25	14.65	3.47	—	—	—	1.18	0.15
<b>e_Ti-spinel (TiO<sub>2</sub>-CaSiTiO<sub>5</sub>)</b>	23.90	6.79	15.13	3.87	1.17	0.23	48.89	—	—	—

TABLE 6

Results of EDS analysis on reformed slag samples with CaO additives of from 10 to 25 wt.%

Element, wt.%	O	Si	Ca	Al	Mg	Na	Mn	K	Ba	S
<b>Reformed slag with 10 wt.% CaO additives</b>										
<b>Matrix_Anorthite(Na)</b>	40.21	20.77	22.46	10.07	2.45	1.88	0.58	0.78	0.80	—
<b>Solid-phase_Anorthite</b>	41.43	21.42	19.32	11.03	6.80	—	—	—	—	—
<b>Reformed slag with 15 wt.% CaO additives</b>										
<b>Matrix_Anorthite + Wollastonite</b>	40.86	20.90	28.41	6.87	0.22	—	0.45	0.31	1.77	0.22
<b>Solid-phase_Melilite</b>	40.35	16.77	28.41	9.86	3.97	0.64	—	—	—	—
<b>Reformed slag with 20 wt.% CaO additives</b>										
<b>Solid-phase_Melilite</b>	42.24	17.88	25.79	8.58	4.12	1.40	—	—	—	—
<b>Matrix_Anorthite</b>	44.22	21.50	19.20	10.98	0.62	0.49	0.41	0.71	1.60	0.28
<b>Reformed slag with 25 wt.% CaO additives</b>										
<b>Solid-phase_Melilite</b>	41.37	16.50	27.46	9.78	4.03	0.86	—	—	—	—
<b>Matrix_Anorthite + Wollastonite</b>	42.52	20.82	25.51	8.22	0.37	0.20	0.35	0.31	1.39	0.31



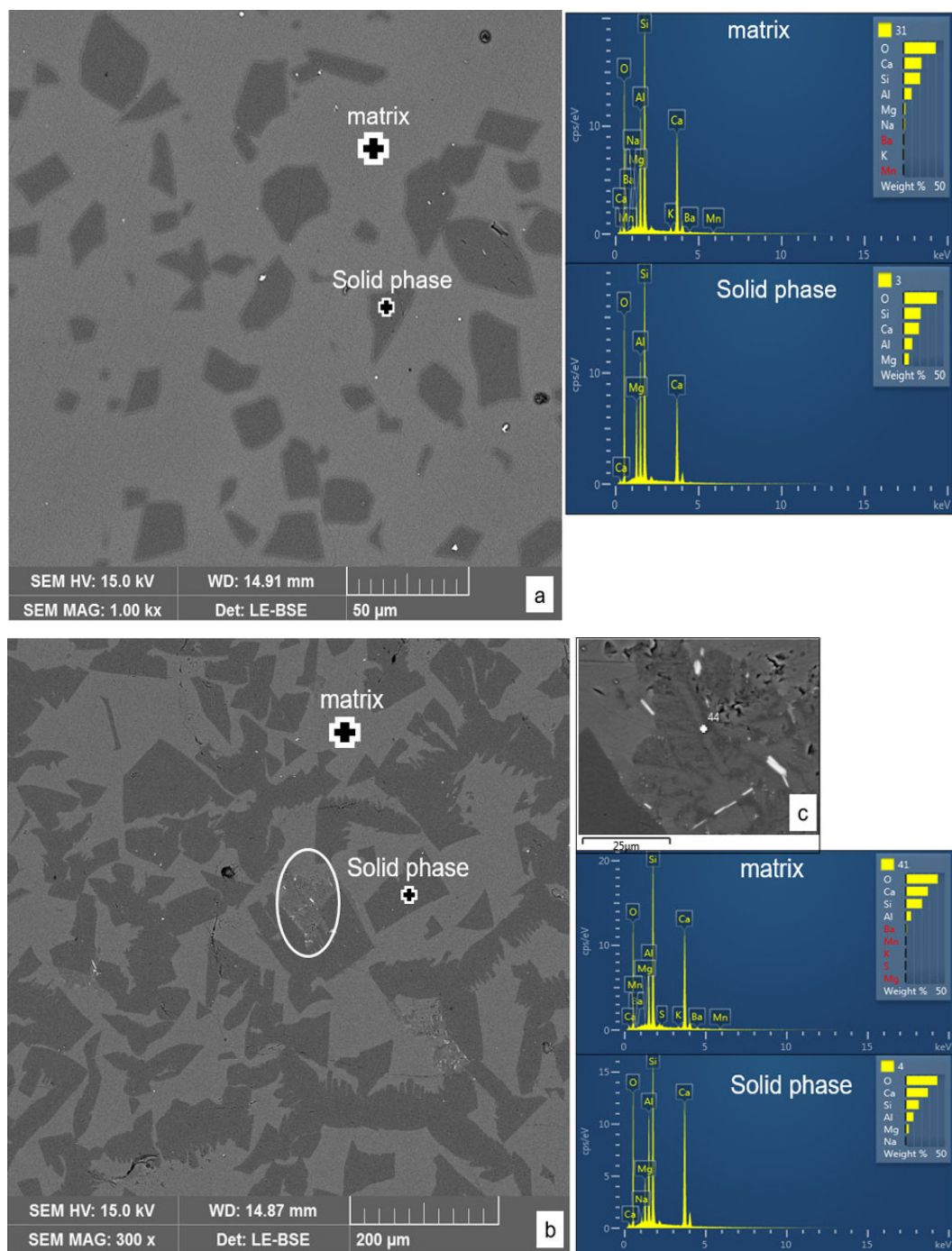


Fig. 7. SEM images and EDS micrographs of reformed slag samples: (a) sample with 10 wt.% CaO additives; (b) sample with 15 wt.% CaO additives; (c) zoom-in image of the sample with 15 wt.% CaO additives

are of 15 wt.%, the shape of the solid-phases was changed to other irregular shapes with exhibited greater size and transformed from anorthite to the melilite again, as shown in Fig. 7(b) and Table 5. The melilite is a complex solid formed by akermanite  $\text{Ca}_2\text{Mg}(\text{Si}_2\text{O}_7)$  and gehlenite  $\text{Ca}_2\text{Al}(\text{AlSiO}_7)$  [18], it was confirmed according to XRD results. The zoom-in figure (Fig. 7(c)) shows that mixtures of solid-phase (melilite + anorthite + wollastonite + Barium's spinel) existed next to solid-phase with irregular quadrilateral. EDS results indicated that the matrix was also transformed to kind of the anorthite and wollastonite, has been contained 0.22 wt.% of sulphur, as shown in Table 6.

With CaO additives of 20 wt.% and 25 wt.%, the matrices were anorthite has been still dissolved the sulphur of 0.28 wt.% and 0.31 wt.%, respectively (Fig. 7 (d) and (e), and Table 6). The solid-phases are also represented by melilite form with different irregular shape and size, but mixtures (melilite + anorthite + wollastonite + Barium's spinel) observed in the slag sample with CaO addition of 25 wt.%. According to EDS analysis, anorthite and wollastonite phases dissolved the sulphur, which indicates that sulphide has been incorporated into the anorthite and wollastonite phases.



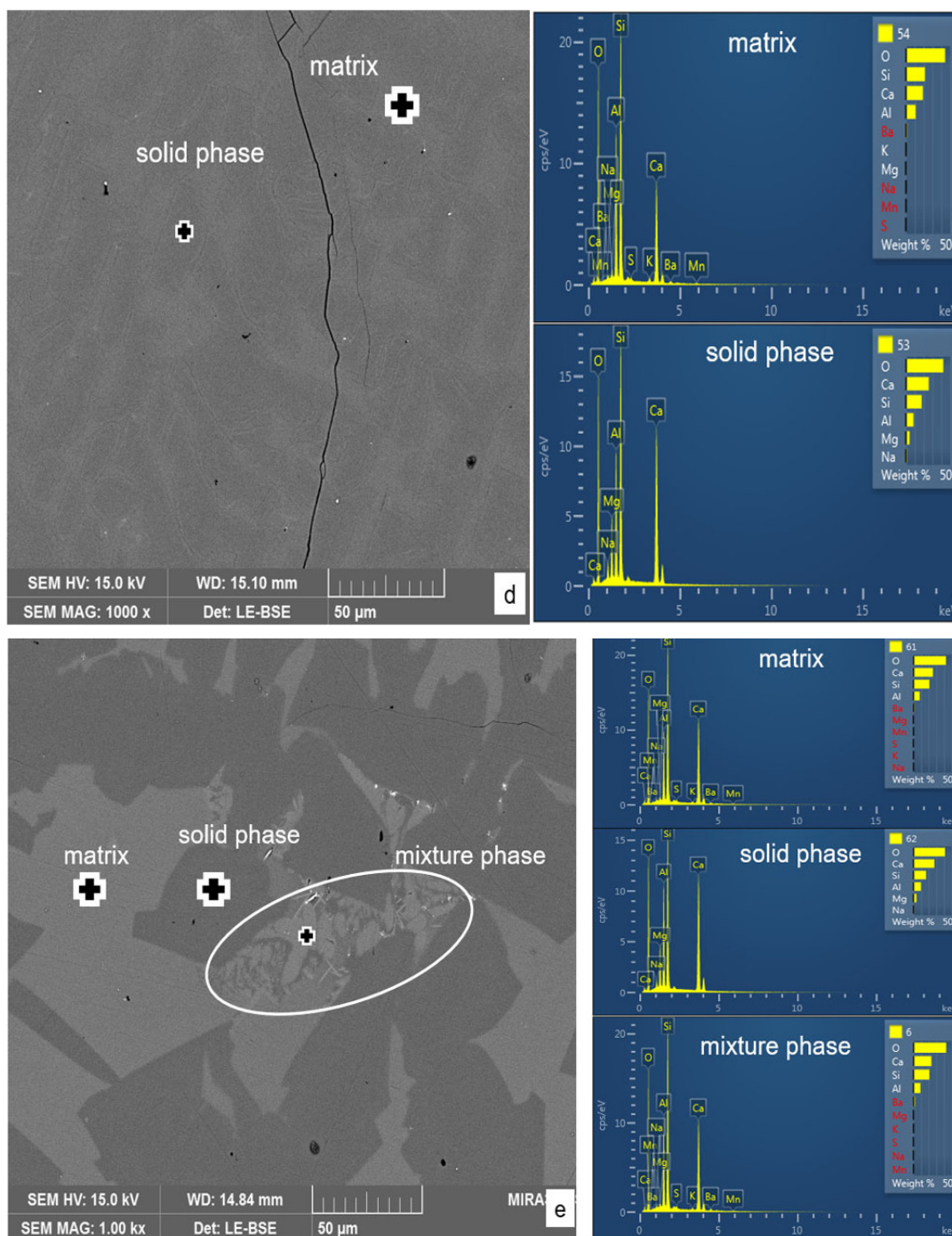


Fig. 7. SEM images and EDS micrographs of reformed slag samples: (d) sample with 20 wt.% CaO additives; (e) sample with 25 wt.% CaO additives

#### 4. Conclusions

The feasibility of a high-temperature reduction technology to improve beneficiation of metallic elements and reformed slag during pig iron recovery from copper slag was investigated. The following conclusions were obtained.

- Iron in the copper slag was completely reduced and separated through iron alloy at the temperature of 1600°C and the holding time of 30 minutes using the reduction smelting as well as the copper in the copper slag was also dissolved into the pig iron during the reduction smelting. The pig iron

contained about 3 wt.% of copper that it is possible to use at the cast iron containing copper for excellent casting alloys have significant properties including strength, toughness and corrosion resistance, and etc.

- Changes of the chemical composition of the reformed slag are highly dependent on the CaO additives, and acid kind of the reformed slag without CaO additives transformed to the basic slag, which slag basicity reached from 1.05 to 2.9, due to increasing CaO concentration in the reformed slag. When CaO additives were 10 and 20 wt.%, the chemical compositions of reformed slag were similar with Blast-

Furnace slag, which it is potentially replacement in raw material of Portland cement.

- The XRD analysis of reformed slag indicated that the reformed slag without CaO additives was glass-like slag, but reformed slags with CaO additives were calcium silicate type slag. The main phases in the reformed slag with CaO additives were determined to be several compounds as akermanite-gehlenite series.
- The SEM-EDS analysis showed that reformed slag without CaO additives was like glass matrix, and tested as the pyroxene phase  $(Ca,Na)(Al,Mg)(Al,Si)_2O_6$  according to the EDS analysis and ternary oxide system of  $Al_2O_3$ -CaO-SiO<sub>2</sub>. In the reformed slags with CaO additives, various solid-phases with different size and shape, and matrix are observed, and matrix and solid-phases mainly existed melilite and anorthite structure. At 10 wt.% of CaO additives, modification effects appeared that the shapes of the solid-phase were changed to other irregular shapes with exhibited greater size.

#### Acknowledgement

This study was supported by the BB21+ Project in 2020 and co-supported under Grant No. NRF2019R1F1A104940 by the National Research Foundation of Korea (NRF), funded by MSIT of the Republic of Korea.

#### REFERENCES

- [1] LS-Nikko copper inc., Private Communication. 2012 Ulsan, Korea.
- [2] Korea Zinc Co., Ltd., Onsan Refinery, Private Communication. 2012 Ulsan, Korea.
- [3] S.W. Ji, C.H. Seo, J. of Korean Inst. of Resources Institute. **2**, 68-72 (2006).
- [4] J.P. Wang, K.M. Hwang, H.M. Choi. *Indian J. Appl. Res.* **2**, 977-982 (2018).
- [5] J.P. Wang, K.M. Hwang, H.M. Choi. *Indian J. Appl. Res.* **2**, 973-976 (2018).
- [6] A.A. Lykasov, G.M. Ryss, *Steel Trans.* **46** (9), 609-613 (2016).
- [7] M.K. Dash, S.K. Patro and etc., *Int. J. Sustain. Built. Environ.* **5**, 484-516 (2016).
- [8] B. Gorai, R.K. Jana and etc., *Resour. Conserv. Recy.* **39**, 299-313 (2003).
- [9] I. Alp, H. Deveci, H. Sungun. *J. Hazard. Mater.* **159**, 390-395 (2008).
- [10] P. Sarfo, G. Wyss and etc., *J. Min. Eng.* **107**, 8-19 (2017).
- [11] U. Yuksel, I. Tegin. *J. Environ. Sci. Eng. Technol.* **6**, 388-394 (2017).
- [12] Z.X. Lin, Z.D. Qing and etc. *ISIJ Int.* **55**, 1347-1352 (2015).
- [13] Z. Guo, D. Zhu and etc., *J. Met.* **86** (6), 1-17 (2016).
- [14] A.A. Lykasov, G.M. Ryss and etc., *Steel Transl.* **46** (9), 609-613 (2016).
- [15] Z. Cao, T. Sun and etc., *Minerals.* **6** (119), 1-11 (2016).
- [16] A.Es. Nassef. A. Abo Ei-Nasr, Influence of Copper Additions and Cooling Rate on Mechanical and Tribological Behavior of Grey Cast Iron, 7<sup>th</sup> Int. Saudi Engineering Conference (SEC7), KSA, Riyadh 2-5, 2-5 Dec 2007, p. 307
- [17] G. Gumienny, B. Kacprzyk, *Arch. Foundry Eng.* **17**, 51-56 (2017).
- [18] Z. Slovic, K.T. Raic, L. Nedeljkovic, etc., *Mater. Technol.* **46** (6), 683-688 (2012).
- [19] U. Erdenebold, H.M. Choi. J.P. Wang. *Arch. Metal. Mater.* **63** (4), 1793-1798 (2018).
- [20] Ye.A. Kazachkov, Calculations on the theories of metallurgical processes. Metallurgy, Moscow (1988).
- [21] G.I. Silman, V.V. Kamynin and etc., *Met. Sci. Heat. Treat.* **45** (2003), 254-258.
- [22] A.A. Razumakov, N.V. Stepanova and etc., Proceedings of MEACS2015. IOP conference series: materials science and engineering, Tomsk Polytechnic University, Tomsk, 1-4 December 2015, **124**, 012136 (2016).
- [23] E. Konca, K. Tur and etc., *Metals* **7** (320), 1-9 (2017).
- [24] J.O. Agunsoye, S.A. Bello and etc., *J. Miner. Mater. Character. Eng.* **2**, 470-483 (2014).
- [25] A.A. Rahman, S.A. Abo-El-Enein and etc., *Arab. J. Chem.* **9**, 8138-8143 (2016).
- [26] D.E. Angulo-Ramirez, R.M. de Gutierrez and etc., *Constr. Build. Mater.* **140**, 119-128 (2017).
- [27] Y. Maeda. Nippo steel and Sumitomo metal technical report. **109**, 114-118 (2015).
- [28] Y. Ueki. Nippo steel and Sumitomo metal technical report. **109**, 109-113 (2015).
- [28] <https://www.snmnews.com/news/articleView.html?idxno=447525>, accessed: 05.06.2019.
- [39] M. Fleischer. Geological survey professional paper 440-L, 6th edition. Washington, 1964, p. 21-23.
- [31] Verlag Stahleisen GmbH. Slag atlas. 2nd edition, Germany, 1995, p. 127.